ISSN 1027-5495. Functional Materials, 29, No.3 (2022), p. 338-345.
doi:https://doi.org/10.15407/fm29.02.338 © 2022 — STC "Institute for Single Crystals"

Features of pseudoisocyanine J-aggregates formation in spin-assisted layer-by-layer assembled films and their interaction with metal nanoparticles

I.I.Grankina, I.I.Bespalova, S.L.Yefimova, A.V.Sorokin

Institute for Scintillation Materials, National Academy of Sciences of Ukraine, 60 Nauky Ave., 61072 Kharkiv, Ukraine

Received June 22, 2022

Features of pseudoisocyanine J-aggregates formation in layer-by-layer assembled polymer films by the spin-assisted method were studied by optical spectroscopy. The films prepared by the spin-assisted LbL method appeared to be thicker and more inhomogeneous compared with those prepared by the sprayed LbL method. As a result, a large topological disorder causing weaker dipole-dipole interaction was revealed for the J-aggregates. Plasmon enhancement of the J-aggregates luminescence by gold and silver nanoparticles was studied. Due to PIC J-aggregates features in spin-assisted LbL films the luminescence enhancement by gold NPs appeared to be less efficient compared to the J-aggregates in sprayed LbL films. However, due to the H-band of PIC J-aggregates, the luminescence enhancement by silver NPs was achieved despite the large spectral distance between the corresponding plasmon band and J-band.

Keywords: J-aggregate, metal nanoparticle, layer-by-layer assembly, exciton, plasmon, luminescence.

Особливості формування псевдоізоціанінових J-агрегатів у спин-ассистованих пошарово зібраних плівках та їх взаємодія з наночастинками металів. *І.І.Гранкіна, І.І.Беспалова, С.Л.Єфімова, А.В.Сорокін*

Методом оптичної спектроскопії досліджено особливості формування J-агрегатів псевдоізоціаніну у пошарово зібраних полімерних плівках із застосуванням методу нанесення центрифугуванням. Плівки, отримані за допомогою методу LbL з центрифугуванням, виявилися більш товстими та більш неоднорідними порівняно з плівками LbL, отриманими напиленням. В результаті для J-агрегатів було виявлено великий топологічний безлад, що спричиняє слабшу диполь-дипольну взаємодію. Досліджено плазмонне підсилення люмінесценції J-агрегатів наночастинками золота та срібла. Через особливості J-агрегатів PIC у плівках LbL з центрифугуванням, підсилення люмінесценції золотими НЧ виявилося менш ефективним порівняно з J-агрегатами в напилених плівках LbL. Однак завдяки H-смузі J-агрегатів PIC було досягнуто підсилення люмінесценції срібними НЧ, незважаючи на велику спектральну відстань між відповідними плазмонною смугою та J-смугою.

1. Introduction

Highly-ordered molecular aggregates, called J-aggregates, reveal many unique spectral properties, like narrow bands, near-resonant luminescence, very short lifetimes, giant oscillator strength, and others [1, 2]. This is caused by the delocalization of the electronic excitations over molecular chains with the formation of Frenkel-type excitons [3]. As the molecules within the J-aggregates are coupled non-covalently, one can affect the spectral properties of J-aggregates by changing their environment [1–3].

For example, in polymer films, J-aggregates often reveal much more stability compared to the aqueous solutions but simultaneously show quenched luminescence due to interaction with a more rigid environment [4].

One of the ways to enhance the J-aggregate luminescence is the interaction with localized surface plasmon resonances of metal nanoparticles [5–9]. Indeed, it is known that nanoparticles (NP) of noble metals show an extraordinary ability to affect the electromagnetic field on a nanometer scale [10–16]. They receive their unique optical properties by being able to maintain the collective oscillations of their electrons in the conduction band known as localized surface plasmon resonances. The appearance of plasmon resonances leads to a significant increase in the density of the local electromagnetic field around the NP, which makes it possible to influence the optical properties of luminophores [10–16].

However, to obtain the maximum luminescence enhancement one needs to place the luminophore and the metal NPs at the optimal distance, which is typically up to 20 nm only [5–13]. One of the ways to achieve such very fine positioning is the layer-by-layer assembly (LbL) of oppositely charged polyelectrolytes [5–9, 12, 13]. Indeed, the LbL allows forming of very thin polymer multilayer composites with a layer thickness of about 1.5 nm only [17–19]. As a result, the LbL approach was successfully applied for plasmon-enhancement of the J-aggregate luminescence [4–9].

However, the disadvantage of the classical method LbL is its considerable duration, because obtaining each layer requires immersion of the sample in an aqueous solution containing the necessary components for at least 30 minutes [4, 17, 20]. Several ways were proposed to accelerate multi-layered film preparation by LbL: spraying [21], rapid agitation of solutions (approximately 1000 rev/min) [22], and spin-assisted LbL [23, 24]. The first approach requires significant consumption of substances and it is difficult to ensure uniform distribution of the film on the substrate [21]. The second way also requires large volumes of solutions to ensure a uniform laminar flow of the substance [22]. Therefore, for the rapid formation of polymer films, we decided to test the spin-assisted layer-by-layer assembly method [23, 24], which has not yet been used to form J-aggregates.

In the present work, we have studied how LbL films formation by spin-assisted method influences pseudoisocyanine (PIC) J-aggregates spectral properties and the efficiency of luminescence enhancement by gold and silver NPs.

2. Experimental

Pseudoisocyanine (PIC, 1,1′-diethyl-2,2′-cyanine iodide,) dye, anionic polyelectrolyte poly(sodium 4-styrenesulfonate) (PSS, average M_w ~ 70000 g/mol, powder), cationic polyelectrolyte poly(diallyldimethylammonium chloride) (PDDA, average M_w < 100000 g/mol, solution 35 wt. % in H_2O,), tetrachloroauric acid ($HAuCl_4$, 99.99 % trace metals basis, 30 wt. % in dilute HCl) and trisodium citrate dihydrate ($Na_3C_6H_5O_7$–$2H_2O$) were purchased from Sigma Aldrich (USA) and used as-received.

PIC J-aggregates were prepared by dissolving the dye PIC (0.5 mM) in an aqueous NaCl (0.2 M) solution under moderate heating (< 80°C). Then the solution was slowly cooled down to room temperature. Gold and silver nanoparticles were synthesized using the well-known Turkevich method according to previously published procedures [6, 7]. The sprayed method of LbL film preparation was described in [7]. To prepare polymer films containing the J-aggregates and metal NPs by spin-assisted LbL were used centrifuge MSC 3000 (Biosan, Latvia) with a homemade substrate holder. A substrate glass plate was preliminarily cleaned with hot (95°C) piranha acid ($H_2SO_4 + H_2O_2$ = 2:1) which gives the glass surface of negative charge. Then, an aqueous polycation PDDA solution (2 wt. %) was dropped on the substrate mounted in the centrifuge holder and spread over the whole substrate surface. Then, the substrate was rotated at 2000 rpm for 3 min forming a thin positively charged polymer layer. Each layer deposition was followed by rinsing sprayed distilled water to remove loosely adsorbed species. The next layer was formed in the same way using the water solution of metal NPs stabilized with citrate anions that imply the negative charges [6, 7]. A PDDA layer was deposited on the metal NPs layer with the successive deposition of a negatively charged polymer layer from an aqueous polyanion PSS solution (2 wt. %). As PIC dye is the cationic one, the J-aggregates layer was deposited on the PSS layer or directly on the layer containing NPs. To control the distance between metal NPs and PIC J-aggregates, the PDDA and PSS layers were alternated. The J-aggregates layer was

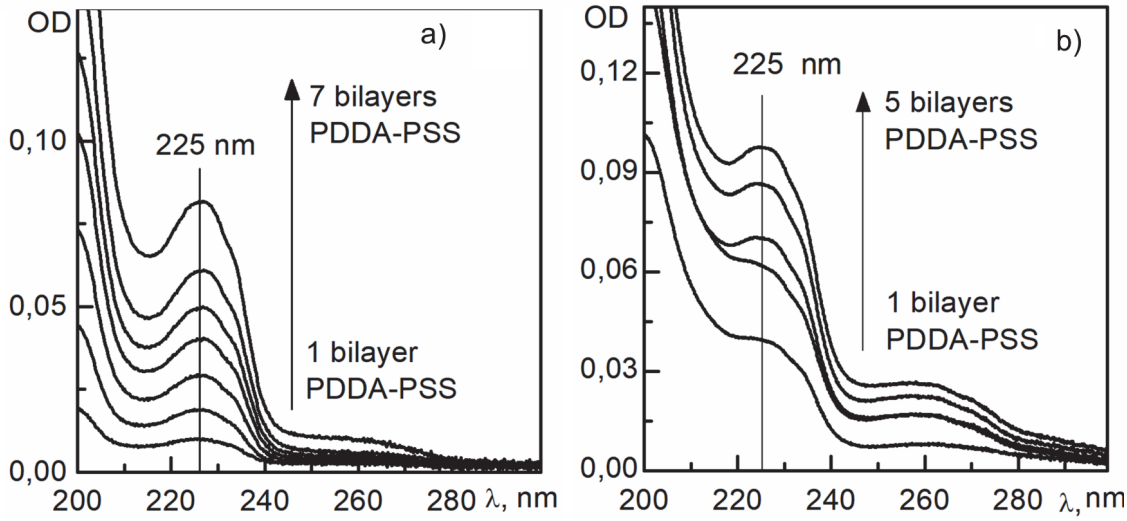

Fig. 1. Absorption spectra of polymer films deposited by the sprayed (a) and spin-assisted (b) LbL methods for different numbers of PDDA-PSS bilayers.

coated by PSS one to provide isolation from surrounding air [7, 9].

Absorption spectra at room temperature were registered using spectrophotometer Specord 200 (Analytik Jena, Germany). Luminescence spectra were registered using spectrofluorimeter Lumina (ThermoScientific, USA). Luminescence image of the polymer film was obtained using a fluorescent microscope MIKMED-2 var.11 (LOMO) coupled with a 10 Mp microscope digital camera M3CMOS 10000 (Sigeta, Ukraine). Luminescence was excited at 450–480 nm and collected in the 520–700 nm spectral range. Low-temperature measurements were performed at 80 K using a nitrogen cryostat. In this case, luminescence and absorption spectra were obtained using a fiber-optic microspectrometer USB4000 (OceanOptics, USA) via a homemade fiber-optic adapter attached to the 20^X eyepiece. The spectral output of the microspectrometer USB4000 was calibrated using a calibrated tungsten halogen lamp HL-2000-CAL (OceanOptics, USA). As the luminescence excitation source, an emission at a wavelength of 514 nm of multiline Ar-laser Stellar-PRO ML/150 (ModuLaser, USA) was used. For the absorption spectra, an incandescent lamp was used.

3. Results and discussion

First of all, we will determine whether the spin-assisted LbL method affects the formation of pure polymer films. It is known that the main ways of determining the thickness of polymer films obtained by the LbL method are atomic force microscopy (AFM) and high-resolution optical interferometry [17–19]. However, this can be done using optical absorption techniques also, since polyelectrolyte PSS has a well-defined band with a maximum at $\lambda = 225$ nm [23, 24]. Thus, we compared the absorption spectra of PDDA-PSS bilayers deposited on a quartz substrate, depending on the number of corresponding bilayers both for sprayed and spin-assisted LbL methods (Fig. 1).

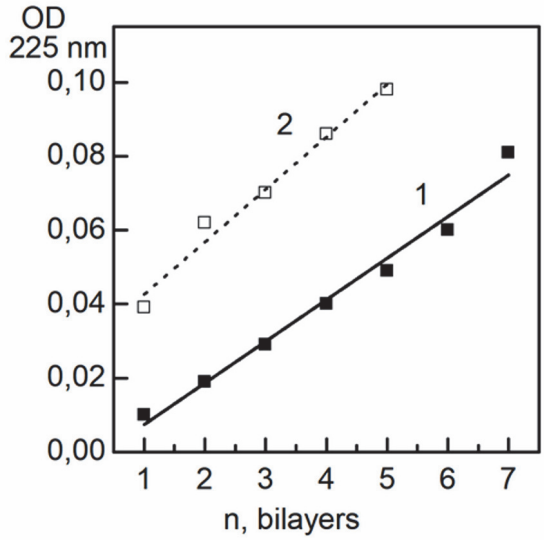

Fig. 2. Dependence of film absorption at $\lambda = 225$ nm on the number of bilayers for sprayed (*1*) and spin-assisted (*2*) LbL methods.

When comparing the absorption spectra in the UV range of the spectrum, one can see the growth of the absorption band with a maximum at $\lambda = 225$ nm (Fig. 1). For the spin-assisted method, the intensity of absorption is higher compared to the sprayed

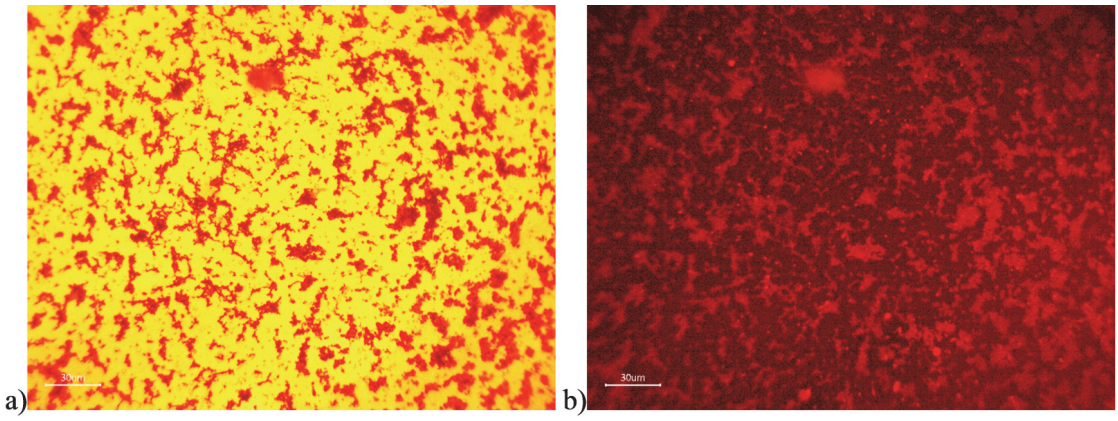

Fig. 3. Microscopic images of PIC J-aggregates in the spin-assisted LbL film: a) in the transmitted light, b) luminescent image. Scale bar is 30 μm.

LbL method (Fig. 1). With the uniform sequential deposition of the films, we must obtain a linear dependence of PSS films absorption intensity at $\lambda = 225$ nm on the number of the layers [23, 24]. Indeed, for both film deposition methods, we get such linear dependence (Fig. 2).

For the sprayed LbL method, the dependence of the film absorption at $\lambda = 225$ nm on the number of bilayers is described by a line passing through zero point and having a slope of 0.011 (Fig. 2, curve 1). Thus, for each bilayer, the optical density increases by 0.011. As the thickness of the bilayer is approximately 3 nm (each layer of PDDA and PSS is approximately 1.5 nm [6, 7, 17–19]), therefore each 1 nm of polymer film thickness gives an optical density of ~ 0.0035.

For the spin-assisted LbL method the dependence of the film absorption at $\lambda = 225$ nm is also described by a straight line (Fig. 2, curve 2), but it intersects the Y axis at the point OD ~ 0.028 (for $n = 0$) and its slope is 0.014. This means that, firstly, the first bilayer of the films is formed too thick (approximately 12 nm), and secondly, the thickness of all other bilayers of PDDA-PSS is approximately 4 nm, i.e. 30 % thicker compared to sprayed LbL. How will such features of spin-assisted polymer film formation affect the PIC J-aggregates spectral properties?

Similar to previously reported results for PIC J-aggregates in sprayed LbL films [25], the J-aggregates in spin-assisted LbL films demonstrate a two-dimensional island-like morphology (Fig. 3).

In contrast to the microscopic images, the absorption spectra have shown the difference between PIC J-aggregates in LbL

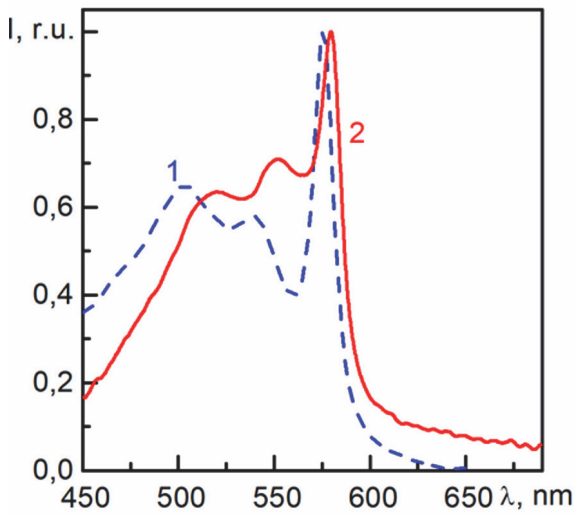

Fig. 4. Absorption spectra of PIC J-aggregates formed in LbL films by sprayed (*1*) and spin-assisted (*2*) methods at room temperature.

films formed by different methods (Fig. 4). In the spin-assisted film the J-band ($\lambda^{J}_{\max}$ = 580 nm), the monomer band ($\lambda^{mon}_{\max}$ = 551.5 nm) and the H-band ($\lambda_{max}{}^{H}$ = 520 nm) are red-shifted compared to ones ($\lambda^{J}_{\max}$ = 575.5 nm, $\lambda^{mon}_{\max}$ = 540 nm and $\lambda^{H}_{\max}$ = 503 nm, respectively) in sprayed film (Fig. 4). The spectral shift for monomer and excitonic bands has different nature. While the red shift of the monomer band reflects the changes in its solvation shell (so-called solvatochromic effect [26, 27]), the excitonic bands' shift reflects changing the dipole-dipole strength J, which could be found as [3]:

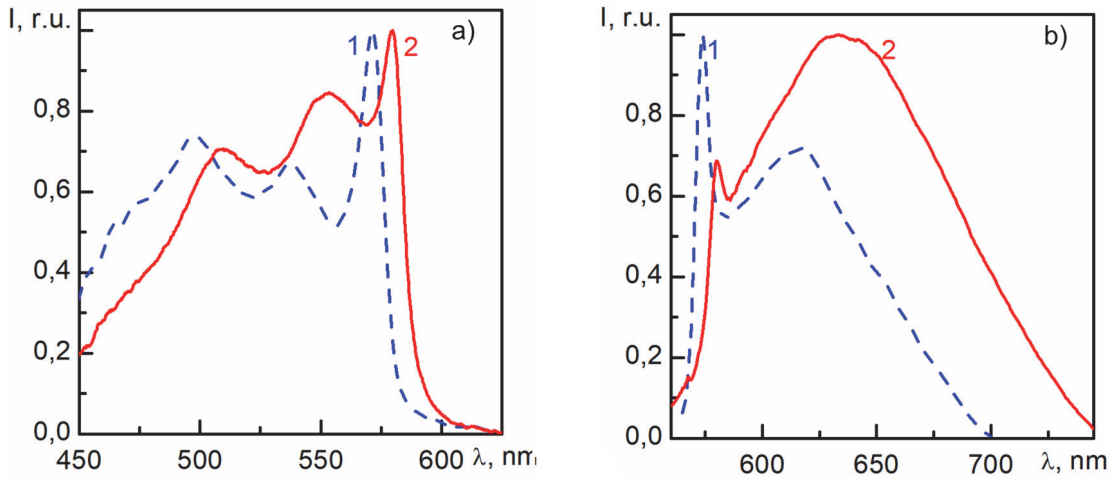

Fig. 5. Absorption (a) and luminescence (b, λ_{exc} = 514 nm) spectra of PIC J-aggregates formed in LbL films: *1* — by the sprayed method, *2* — by the spin-assisted method. T = 80 K.

$$J = \frac{\nu_{mon} - \nu_J}{2.4}, \quad (1)$$

where ν_{mon} and ν_J are maxima of the monomer band and the J-band expressed in cm^{-1}, respectively. The dipole-dipole strength can be estimated for PIC J-aggregates in sprayed LbL film as J_{spr} ~ 470 cm^{-1} and in spin-assisted LbL film as J_{sa} ~ 230 cm^{-1}. Thus, in the spin-assisted film, the PIC J-aggregates reveal two-times weaker dipole-dipole strength.

Also, the J-band in the spin-assisted film reveals a significant contribution to the long-wavelength edge (Fig. 4, curve 2). The latter is a signature of the larger topological static disorder [3, 25, 28]. As it is known, the static disorder, which includes energy and topological ones, leads to a decrease in the exciton coherence length [3, 25, 28], which can be estimated using the equation:

$$N_{coh} = \frac{3\cdot(\Delta\nu^{mon}_{FWHM})^2}{2\cdot(\Delta\nu^{J}_{FWHM})^2} - 1, \quad (2)$$

where $\Delta\nu^{mon}_{FWHM}$ and Δ^{J}_{FWHM} full widths at the half maxima of the monomer band and J-band, respectively. For the J-band in the studied films $\Delta\nu^{J}_{FWHM}$ = 330 cm^{-1} for both cases, so taking into account $\Delta\nu^{mon}_{FWHM}$ = 990 cm^{-1} [25] the exciton coherence lengths are N_{coh} ~ 15. The similarity of the exciton coherence length means that the energy disorder, which makes the main contribution to the J-band width, is the same for the J-aggregates in both types of films. Thus, the topological disorder manifests itself mainly in the growth of the long-wavelength tail of the J-band. A possible reason for its increase can be weakening the strength of the dipole-dipole interaction in the J-aggregates formed in spin-assisted films.

The growth of the topological disorder can lead to increasing the exciton-phonon interaction and the efficiency of the exciton self-trapping in J-aggregates [25, 28]. Indeed, at low temperature (T = 80 K) one can see (Fig. 5b, curve 2) that in the spin-assisted film the long-wavelength luminescence band (λ^{ST}_{max} = 635 nm) of PIC J-aggregates, which corresponds to the emission of self-trapped excitons, is much higher in intensity than the free-exciton band (λ^{FE}_{max} = 580 nm).

Additionally, the Fig. 5a shown that the red-shift for the absorption bands (λ^{J}_{max} = 579.5 nm, λ^{mon}_{max} = 553 nm and λ^{H}_{max} = 509 nm) of the J-aggregates in spin-assisted film compared to those (λ^{J}_{max} = 571 nm, λ^{mon}_{max} = 537 nm and λ^{H}_{max} = 497 nm) in sprayed films is larger than at room temperature (Fig. 4). According to Eq. 1, we can estimate the dipole-dipole strength for PIC J-aggregates in sprayed LbL film as J_{spr} ~ 460 cm^{-1} and in spin-assisted LbL film as J_{sa} ~ 345 cm^{-1}. Comparing with the results obtained at room temperature (J_{spr} ~ 470 cm^{-1} and J_{sa} ~ 230 cm^{-1}, respectively), we can conclude that the dipole-dipole strengths are nearly the same for the J-aggregates formed in LbL film by sprayed

method at the different temperatures, while in spin-coated films the strength is larger at low temperature. Thus, the stronger red-shift found for PIC J-aggregates' bands in spin-assisted films (Fig. 5a, curve 2) can be associated primarily with the red-shift of the monomer band. One of the possible reasons for various spectral positions of the PIC monomer bands in different films depending on the temperature is stronger inhomogeneity in spin-assisted films compared with films formed by sprayed method [26, 29]. We can assume, that such inhomogeneity leads to larger topological disorder found for PIC J-aggregates formed in spin-assisted LbL films.

Understanding the exciton properties of PIC J-aggregates formed in spin-assisted LbL films we can analyze the plasmon enhancement of the J-aggregate luminescence by metal nanoparticles. Similarly to previously reported studies [7], the gold NPs have an average size of 20 nm and the maximum of their plasmon resonance (λ_{max}^{Au} = 530 nm) is located at a small spectral distance from the J-band of PIC aggregates (λ_{max}^{J} = 580 nm), as shown in Fig. 6. Moreover, due to its spectral width, the plasmon resonance band of gold NPs shows a good intersection with all bands, which are characteristic for PIC J-aggregates, both exciton and monomeric ones (Fig. 6). This determines the effectiveness of exciton-plasmon interaction in this system [7].

As previously [7], to control the distance between the gold NPs and the J-aggregates, they were introduced into the LbL film in the form of layers separated by a given number of polymer layers. As a result, the luminescence intensity of PIC J-aggregates depends on the distance to the gold NPs (Fig. 7a).

As expected, at a close distance to the NPs, the J-aggregates luminescence was quenched due to the nonradiative energy transfer to the NPs [12, 30, 31]. As the distance increases to a certain value, the J-aggregates luminescence intensity increases compared to that in films without NPs (Fig. 7a). At the optimal distance (4 bilayers between J-aggregates and NPs, ~ 16 nm) the coefficient of plasmon enhancement of PIC J-aggregates luminescence is ~ 5. Further distance increase leads to gradual luminescence decreasing to the values characteristic of films in the absence of NPs (Fig. 7a). Note that the luminescence enhancement coefficient is lower than that (~ 8) obtained in LbL films formed by the sprayed

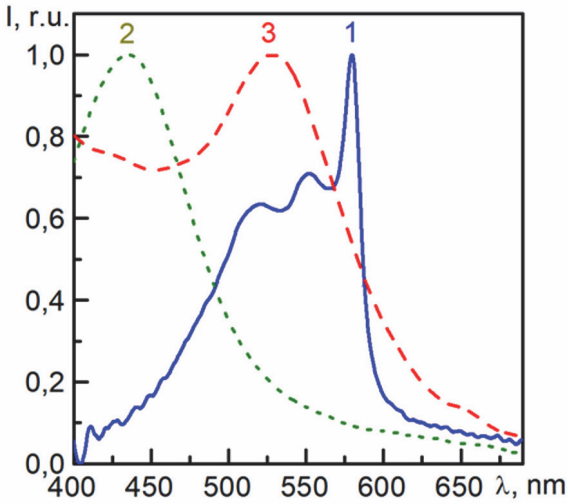

Fig. 6. Normalized absorption spectra of PIC J-aggregates (*1*), silver NPs (*2*) and gold NPs (*3*) in the spin-assisted LbL film at room temperature.

method [7]. We can assign such a result to the larger topological disorder in spin-assisted films. Except for the obvious exciton localization, it causes weaker dipole-dipole interaction resulting in a redshift of the excitonic bands. An additional reason can be the red-shift of the PIC monomer band in the spin-assisted LbL film. In the recent experiments concerning plasmon enhancement of TDBC J-aggregate luminescence by gold NPs, we have found an unexpectedly low enhancement coefficient ~ 2.3 [32]. As one of the reasons for such a result, a small intersection of plasmon and exciton bands was supposed [32]. As in the spin-assisted LbL films, PIC J-aggregates bands are red-shifted the cross-section of plasmon and exciton bands becomes smaller leading to decreasing luminescence enhancement coefficient according to the theoretical model proposed in [7]. To prove it, specially designed metal NPs are needed with the plasmon band spectral position much better coinciding with the J-aggregates exciton bands.

Some argumentation to the model can be added if we examine the exciton-plasmon interaction of PIC J-aggregates with silver NPs. Indeed, it is known that the effectiveness of plasmon enhancement of luminescence depends on both the size of metal NPs and their composition [10–16]. Therefore, silver NPs with a size of 50–70 nm are more efficient than gold NPs with a size of 15–20 nm [10–16]. On other hand, the maximum of the plasmon resonance for sil-

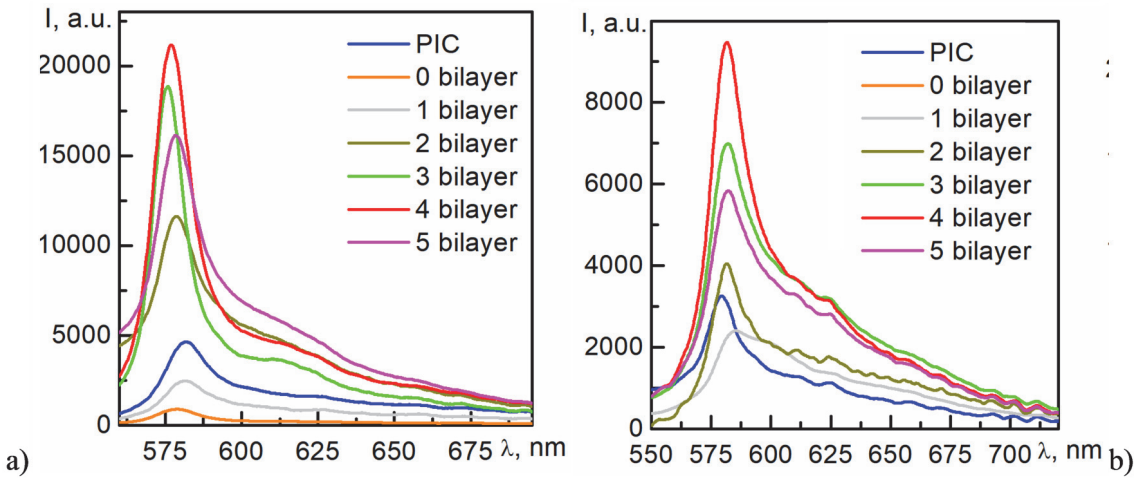

Fig. 7. Dependence of PIC J-aggregates luminescence on the number of PDDA-PSS bilayers between them and gold (a) and silver (b) nanoparticles. For comparison, films without NPs are also shown.

ver NPs with a size of 50 nm λ_{max}^{Ag} = 435 nm [6] is located at a significant spectral distance from the J-band of PIC J-aggregates (Fig. 6). However, PIC J-aggregates possesses more complicated exciton structure [1, 2, 7, 9, 25] compared to TDBC J-aggregates [32, 33] and their H-band reveal spectral cross-section with plasmon band of silver NPs (Fig. 6). Therefore interesting, if it is sufficient condition for plasmon enhancement of PIC J-aggregates' luminescence by silver NPs?

Despite the much smaller spectral cross-section of the plasmon band of silver NPs and H-band of PIC J-aggregates, there is also a change in the luminescence intensity of PIC J-aggregates depending on the layer thickness between the layers of the J-aggregates and the NPs (Fig. 7b). The optimal distance for luminescence enhancement (4 bilayers between J-aggregates and NP, ~ 16 nm) was the same as for the system with gold NP. However, the coefficient of plasmon enhancement of the J-aggregate luminescence is ~ 3, i.e. less than in the case of gold NPs but similar to that in the case of TDBC J-aggregates and gold NPs. Thus, due to the peculiarity of PIC J-aggregates exciton structure revealing both H- and J-bands the exciton-plasmon interaction can be realized even in the case of a large spectral distance between the J-band and plasmon band of metal NPs.

4. Conclusions

The features of PIC J-aggregates spectral properties and interaction with metal nanoparticles in spin-assisted layer-by-layer assembled polymer films were studied using optical spectroscopy. It was found that spin-assisted LbL films appeared to be thicker and more inhomogeneous compared with LbL films prepared by the sprayed method. As a result, PIC J-aggregates formed in the spin-assisted LbL films reveal stronger topological disorder and, hence, weaker dipole-dipole interaction strength. Thus, despite the fast speed and low materials consumption, spin-assisted method of LbL film preparation cannot be considered suitable for J-aggregates formation.

The plasmon enhancement coefficient of PIC J-aggregates luminescence by gold nanoparticles in spin-assisted LbL films was estimated as ~ 5, which is less than that in sprayed LbL film (~ 8) due to the red-shifts of the monomer and excitonic bands as well as a large topological disorder in the J-aggregates. However, due to the specific exciton structure of PIC J-aggregates revealing both H- and J-bands relatively effective exciton-plasmon interaction with the luminescence enhancement coefficient ~ 3 was found for silver NPs, despite the large spectral distance between its plasmon band and the J-band. Therefore, we can conclude the high importance of the exciton and plasmon bands cross-sections to achieve effective exciton-plasmon interaction.

Acknowledgments. The authors thank the Ukrainian Army for the opportunity to prepare the work for publishing. A.Sorokin expresses sincere gratitude to Dr.Franziska Fennel from the University of Rostock for the invaluable help.

References

1. F.Wurthner, T.E.Kaiser, C.R.Saha-Moller, *Angew. Chemie Int. Ed.*, **50**, 3376 (2011).
2. J.L.Bricks, Y.L.Slominskii, I.D.Panas et al., *Methods Appl. Fluoresc.*, **6**, 012001 (2017).
3. J.Knoester, V.M.Agranovich, in: Thin Film. Nanostructures Electron. Excit. Org. Based Nanostructures, ed. by V.M.Agranovich and G.F.Bassani, v.31 (2003).
4. A.V.Sorokin, S.L.Yefimova, Y.V.Malyukin, in: Encycl. Polym. Sci. Technol., John Wiley & Sons, Inc., Hoboken, NJ, USA (2018).
5. N.V.Pereverzev, I.A.Borovoy, O.O.Sedyh et al., *Funct. Mater.*, **21**, 409 (2014).
6. A.V.Sorokin, A.A.Zabolotskii, N.V.Pereverzev et al., *J. Phys. Chem. C*, **118**, 7599 (2014).
7. A.V.Sorokin, A.A.Zabolotskii, N.V.Pereverzev et al., *J. Phys. Chem. C*, **119**, 2743 (2015).
8. A.V.Sorokin, N.V.Pereverzev, V.M.Liakh et al., *Funct. Mater.*, **22**, 316 (2015).
9. A.V.Sorokin, I.I.Grankina, I.I.Bespalova et al., *J. Phys. Chem. C*, **124**, 10167 (2020).
10. M.I.Stockman, *Opt. Express*, **19**, 22029 (2011).
11. M.I.Stockman, *Phys. Today*, **64**, 39 (2011).
12. Metal-Enhanced Fluorescence, ed. by C.D.Geddes, John Wiley & Sons, Inc., Hoboken, NJ, USA (2010).
13. R.Badugu, J.R.Lakowicz, in: Encycl. Spectrosc. Spectrom., ed. by J.C.Lindon, G.E.Tranter, D.W.Koppenaal, 3rd ed., Elsevier (2017), p.676.
14. M.Bauch, K.Toma, M.Toma et al., *Plasmonics*, **9**, 781 (2014).
15. M.Li, S.K.Cushing, N.Wu, *Analyst*, **140**, 386 (2015).
16. J.Dong, Z.Zhang, H.Zheng et al., *Nanophotonics*, **4**, (2015).
17. Multilayer Thin Films, ed. by G.Decher, J.B.Schlenoff, Wiley-VCH Verlag GmbH & Co. KGaA, Weinheim, Germany (2012).
18. Y.Li, X.Wang, J.Sun, *Chem. Soc. Rev.*, **41**, 5998 (2012).
19. Y.Xiang, S.Lu, S.P.Jiang, *Chem. Soc. Rev.*, **41**, 7291 (2012).
20. G.Decher, *Science*, **80**, 1232 (1997).
21. A.Izquierdo, S.S.Ono, J.-C.Voegel et al., *Langmuir*, **21**, 7558 (2005).
22. Y.Fu, S.-J.Li, J.Xu et al., *Langmuir*, **27**, 672 (2011).
23. J.Cho, K.Char, J.-D.Hong et al., *Adv. Mater.*, **13**, 1076 (2001).
24. S.-S.Lee, J.-D.Hong, C.H.Kim et al., *Macromolecules*, **34**, 5358 (2001).
25. A.V.Sorokin, N.V.Pereverzev, I.I.Grankina et al., *J. Phys. Chem. C*, **119**, 27865 (2015).
26. I.Renge, U.P.Wild, *J. Phys. Chem. A*, **101**, 7977 (1997).
27. J.R.Lakowicz, Principles of Fluorescence Spectroscopy, 3rd ed., Springer US, Boston, MA (2006).
28. Y.V.Malyukin, A.V.Sorokin, V.P.Semynozhenko, *Low Temp. Phys.*, **42**, 429 (2016).
29. E.Leontidis, U.W.Suter, M.Schuetz et al., *J. Am. Chem. Soc.*, **117**, 7493 (1995).
30. K.Saito, *J. Phys. Chem. B*, **103**, 6579 (1999).
31. B.Laban, V.Vodnik, M.Dramicanin et al., *J. Phys. Chem. C*, **118**, 23393 (2014).
32. A.Sorokin, R.Grynyov, I.Grankina et al., in: Proc. 2020 IEEE 10th Int. Conf. "Nanomaterials Appl. Prop. N. 2020 (2020).
33. A.V.Sorokin, I.Y.Ropakova, R.S.Grynyov et al., *Dye. Pigment.*, **152**, 49 (2018).